Acta Crystallographica Section D
Biological Crystallography
ISSN 0907-4449

Structural insights into the broadened substrate profile of the extended-spectrum β-lactamase OXY-1-1 from *Klebsiella oxytoca*

Yu-He Liang,*‡ Rong Gao and Xiao-Dong Su*

State Key Laboratory of Protein and Plant Gene Research and Biodynamic Optical Imaging Center (BIOPIC), Peking University, Beijing 100871, People's Republic of China

‡ Present address: Macromolecular Crystallography Laboratory, National Cancer Institute, Frederick, MD 21702, USA.

Correspondence e-mail: liangyh@pku.edu.cn, xdsu@pku.edu.cn

Received 5 May 2012
Accepted 3 August 2012

PDB Reference: OXY-1-1, 3byd

Klebsiella oxytoca is a pathogen that causes serious infections in hospital patients. It shows resistance to many clinically used β-lactam antibiotics by producing chromosomally encoded OXY-family β-lactamases. Here, the crystal structure of an OXY-family β-lactamase, OXY-1-1, determined at 1.93 Å resolution is reported. The structure shows that the OXY-1-1 β-lactamase has a typical class A β-lactamase fold and exhibits greater similarity to CTX-M-type β-lactamases than to TEM-family or SHV-family β-lactamases. It is also shown that the enzyme provides more space around the active cavity for the R_1 and R_2 substituents of β-lactam antibiotics. The half-positive/half-negative distribution of surface electrostatic potential in the substrate-binding pocket indicates the preferred properties of substrates or inhibitors of the enzyme. The results reported here provide a structural basis for the broadened substrate profile of the OXY-family β-lactamases.

1. Introduction

β-Lactam antibiotics are chemotherapeutic drugs widely used for the treatment of various bacterial infectious diseases (Matagne *et al.*, 1998; Ghuysen, 1991). They kill bacteria by inhibiting peptidoglycan transpeptidases and D-alanyl-D-alanine carboxypeptidases, which are key enzymes in bacterial wall synthesis. However, the extensive or even abusive utilization of β-lactam antibiotics has caused the emergence of antibiotic-resistant bacteria, which has seriously restricted the efficiency of antibacterial chemotherapy using β-lactam antibiotics (Levy, 1994; Davies, 1994). The most common cause of bacterial β-lactam antibiotic resistance is the production of β-lactamases by pathogenic bacteria, which hydrolyze the β-lactam amide bond and thus inactivate the antibiotics (Davies, 1994; Frère, 1995). β-Lactamases can be classified into four classes (A to D) according to their sequence and substrate specificity (Ambler, 1980), among which class A β-lactamases are of the greatest importance because they are the most frequently encountered in clinical isolates. Class A β-lactamases are usually encoded by genes located on transferable plasmids, have variable substrate profiles (Matagne *et al.*, 1998) and were originally named penicillinases because of their substrate specificity. Since the 1980s, the broad use of third-generation cephalosporins has caused the appearance of class A extended-spectrum β-lactamases (ESBLs), which show hydrolytic activity towards several extended-spectrum β-lactam antibiotics such as cefotaxime and ceftazidime (Bradford, 2001). The majority of class A ESBLs belong to the TEM or SHV families, which result from point mutations in the non-ESBL parent enzymes the TEM-1/2 and SHV-1 β-lactamases (Knox, 1995). Besides the TEM-family and SHV-family ESBLs, another group of class A ESBLs have also been

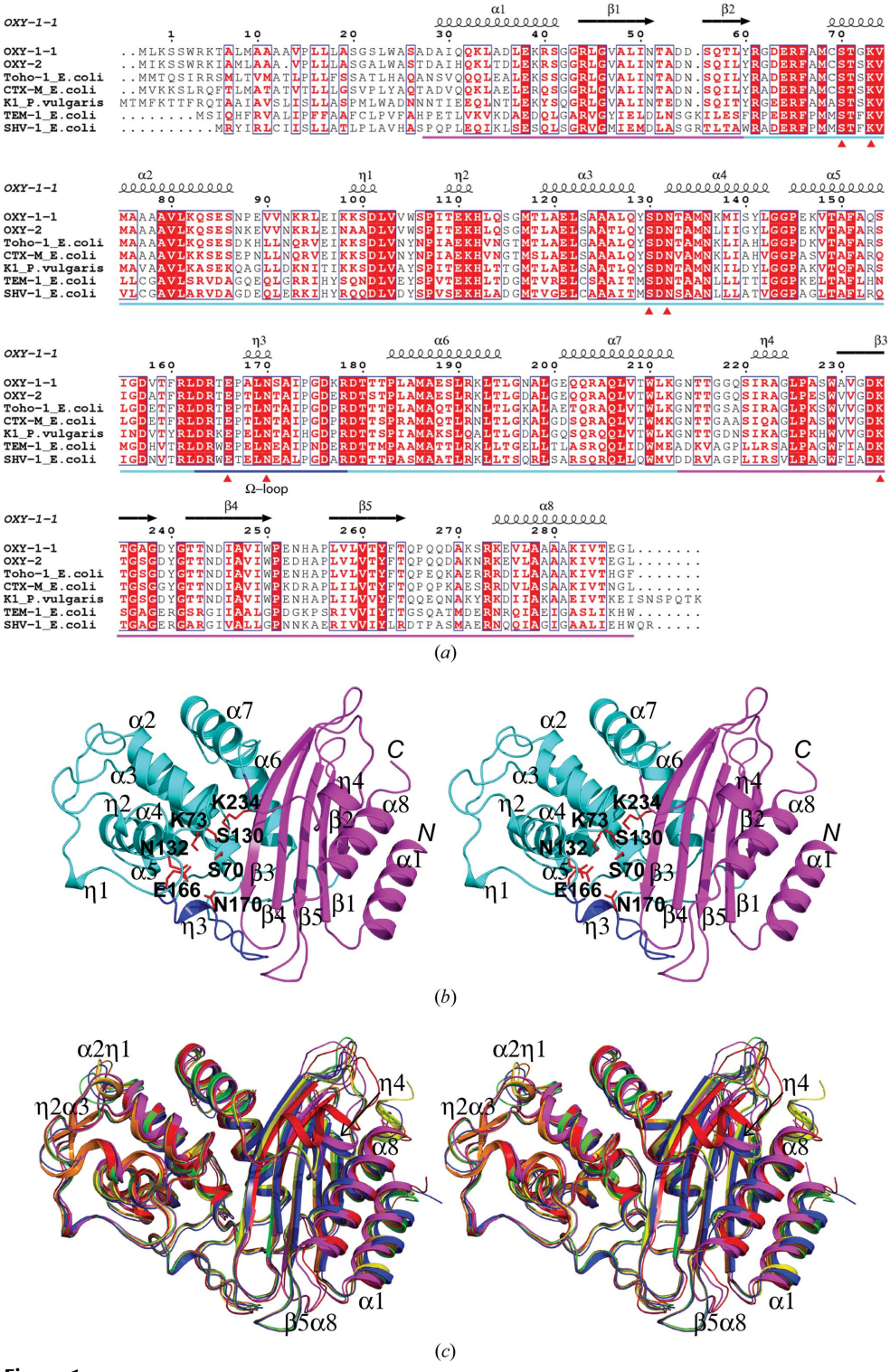

Figure 1
(*a*) Structure-based sequence alignment of OXY-1-1 β-lactamase with five other class A β-lactamases. A red background indicates sequence identity; red letters indicate sequence similarity. Conserved residues with catalytic importance are labelled with red triangles. Magenta, cyan and blue underlining indicates the two domains and the Ω-loop of the enzyme. (*b*) Stereoview showing a ribbon diagram of the OXY-1-1 β-lactamase structure. The α/β and all-α domains are shown in magenta and cyan, respectively. The Ω-loop is shown in blue. Some catalytic important side chains, Ser70, Lys73, Ser130, Asn132, Glu166 and Lys234, are shown as red sticks. (*c*) Stereoview showing the superimposition of the OXY-1-1 β-lactamase structure (this work; green) with *E. coli* Toho-1 (PDB entry 1iys; blue), *E. coli* CTX-M-16 (PDB entry 1ylw; orange), *P. vulgaris* K1 (PDB entry 1hzo; yellow), *E. coli* TEM-1 (PDB entry 1tem; magenta) and *E. coli* SHV-1 (PDB entry 1shv; red) β-lactamase structures. The regions that exhibit significant structural differences are illustrated.

reported that show low sequence identity to the TEM-family and SHV-family members (of around 40%) but have high sequence identity (of greater than 70%) within the group (Bonnet, Sampaio, Chanal *et al.*, 2000; Bonnet, Sampaio, Labia *et al.*, 2000; Poirel *et al.*, 2001; Tzouvelekis *et al.*, 2000). The CTX-M-type β-lactamases, which show strong hydrolytic activity towards cefotaxime, are representative enzymes of this group (Tzouvelekis *et al.*, 2000; Bonnet, 2004).

Klebsiella oxytoca is a pathogen that causes serious infections in hospital patients. It was recognized as being clinically significant in the early 1980s owing to its resistance to β-lactam antibiotics (Podschun & Ullmann, 1998; Hart, 1993). It has been shown that *K. oxytoca* carries chromosomal class A β-lactamase (initially called the K1 β-lactamases and now named OXY β-lactamases) genes (Fournier, Roy *et al.*, 1996). Wild-type *K. oxytoca* produces OXY β-lactamases at a low level constitutively and shows resistance to aminopenicillins and carboxypenicillins (Livermore, 1995). When the OXY β-lactamases are overproduced under induction, the strains resist penicillins, cephalosporins and aztreonam (Fournier *et al.*, 1994). Enzymatic studies showed that the OXY β-lactamases exhibit hydrolytic activity towards cephaloridine, cefuroxime, cefotaxime and aztreonam; this is distinct from the TEM-1/2 and SHV-1 β-lactamases and indicates that the OXY β-lactamases belong to the ESBLs (Wu *et al.*, 1991, 1992; Wu, 1998). Additionally, OXY β-lactamase overproducers are commonly resistant to all combinations of β-lactams with β-lactamase inhibitors (Livermore, 1995). The molecular basis for the overproduction of OXY β-lactamase has been studied using genetic methods. It was shown that the chromosomal

Table 1
Data-collection and structure-refinement statistics.

Values in parentheses are for the highest resolution shell.

Data collection	
Resolution (Å)	55.5–1.93 (1.98–1.93)
Completeness (%)	96.9 (96.1)
R_{merge}† (%)	5.2 (12.9)
Mean $I/\sigma(I)$	30 (10.5)
Space group	$P2_12_12_1$
Unit-cell parameters (Å)	a = 46.54, b = 74.43, c = 84.56
No. of unique reflections	21787
Refinement	
No. of non-H protein atoms	1951
No. of waters	203
No. of ion atoms	20
R_{cryst}‡	0.182 (0.182)
R_{free}§	0.225 (0.283)
Deviations from ideality	
Bond lengths (Å)	0.012
Bond angles (°)	1.236
Average B factors (Å^2)	
All atoms	15.36
Main chain	13.30
Side chain	14.65
Waters	26.08
Ions	41.79
Ramachandran plot statistics (%)	
Most favoured region	90.8
Additional allowed region	8.3
Generously allowed region	0.9

† $R_{merge} = \sum_{hkl}\sum_i |I_i(hkl) - \langle I(hkl)\rangle| / \sum_{hkl}\sum_i I_i(hkl)$. ‡ $R_{cryst} = \sum_{hkl} ||F_{obs}| - |F_{calc}|| / \sum_{hkl} |F_{obs}|$. § R_{free} is the R factor for a selected subset of the reflections which were not included in refinement calculations.

β-lactamase genes in *K. oxytoca* (bla_{oxy} genes) serve as a genetic reservoir of resistant genes and that a high mutation rate in the promoter region causes overproduction of OXY β-lactamases (Fournier, Lagrange *et al.*, 1996*a*,*b*; Fournier *et al.*, 1995). The studies also showed that the OXY β-lactamases can be classified into six groups among which the amino-acid sequence identities are higher than 85% (Fevre *et al.*, 2005; Fournier, Roy *et al.*, 1996; Granier *et al.*, 2003; Wu *et al.*, 1992). Sequence alignment showed that the OXY β-lactamases have higher sequence identity to CTX-M-type β-lactamases than to TEM-type or SHV-type β-lactamases (Fig. 1*a*), indicating that the OXY and CTX-M β-lactamases belong to the same group of class A ESBLs.

All class A β-lactamase structures share a common fold (Matagne *et al.*, 1998) and their enzymatic properties such as substrate specificity and resistance to inhibitors are dependent on the conformation around the active centre. Several structures of CTX-M-type ESBLs (Chen *et al.*, 2007; Chen, Delmas *et al.*, 2005; Chen, Shoichet *et al.*, 2005) have been determined in the apo form, in complexes with different transition-state analogues and in complexes with β-lactam inhibitors, revealing the details of enzymatic catalysis. The structures show that the active-centre volumes of the CTX-M-type ESBLs are similar to those of the non-ESBLs TEM-1 and SHV-1 (around 160 Å^3), while some TEM-family ESBLs, such as TEM-52 (Orencia *et al.*, 2001) and TEM-64 (Wang *et al.*, 2002), have an enlarged active centre that broadens their substrate profile. No structure of an OXY β-lactamase has been determined to date. The structure with the highest sequence identity to OXY β-lactamases is that of the Toho-1 β-lactamase from *Escherichia coli* (Ibuka *et al.*, 1999, 2003; Kimura *et al.*, 2004; Shimizu-Ibuka *et al.*, 2004), which also belongs to the same group as the CTX-M-type ESBLs. In order to study the catalytic mechanism and the extended substrate profiles of OXY β-lactamases, especially their high levels of activity towards both penicillins and cephalosporins upon induction and their resistance to combinations of β-lactams with β-lactamase inhibitors, structural information on the enzymes is indispensable. In this work, the crystal structure of an OXY β-lactamase, OXY-1-1, was determined at 1.93 Å resolution. The structural features that are essential for the broad substrate profile of the enzyme were analyzed. Our results will be beneficial for the design of more efficient and specific β-lactamase inhibitors targeting OXY β-lactamases.

2. Materials and methods

2.1. Protein preparation, crystallization and X-ray data collection

The preparation and crystallization of *K. oxytoca* OXY-1-1 β-lactamase has been described previously (Wu *et al.*, 2004). Briefly, the gene encoding the OXY-1-1 β-lactamase was amplified from chromosomal DNA of *K. oxytoca* KH66 and was expressed in *E. coli* in soluble form with a C-terminal His tag. The recombinant protein was purified and crystallized. Two crystal forms were obtained from the same crystallization buffer consisting of 25%(*w*/*v*) PEG 4000, 0.1 *M* sodium acetate pH 4.5, 0.2 *M* ammonium sulfate. One crystal form was orthorhombic and diffracted to better than 1.9 Å resolution, while the other was tetragonal and diffracted to 3.0 Å resolution. Complete data sets were collected from both crystal forms on beamline I711 at the MAX II synchrotron, Lund, Sweden. The orthorhombic crystal belonged to space group $P2_12_12_1$, with unit-cell parameters a = 46.54, b = 73.43, c = 84.56 Å. The data were processed to 1.93 Å resolution and the statistics of data collection are listed in Table 1.

2.2. Structure determination, validation and illustration

The structure of *K. oxytoca* OXY-1-1 β-lactamase was determined by the molecular-replacement method using the orthorhombic data set. The structure of Toho-1 β-lactamase from *E. coli* (PDB entry 1bza; Ibuka *et al.*, 1999) was used as the search model. Rotation and translation searches were carried out with the program *CNS* (Brünger *et al.*, 1998) using data in the resolution range 15–4 Å. The model was subjected to refinement with TLS restraints (Painter & Merritt, 2006) using the *REFMAC*5 (Murshudov *et al.*, 2011) program in the *CCP*4 suite (Winn *et al.*, 2011). Diffraction data within the resolution range 55.5–1.93 Å were used in refinement and 5% of the reflections were set aside for cross-validation. Manual adjustment of the model was performed with *Coot* (Emsley & Cowtan, 2004). Solvent and ligand molecules were introduced into positive difference density during the final steps of refinement. The quality of the final model was validated using

Table 2
R.m.s.d.s between OXY-1-1 and five other class A β-lactamases.

	R.m.s.d. (Å)	
β-Lactamase	For all C^{α} atoms	For six strictly conserved residues in the catalytic cavity
E. coli TEM-1	1.7	0.220
E. coli SHV-1	2.0	0.275
E. coli Toho-1	0.5	0.524
E. coli CTX-M-16	0.6	0.169
P. vulgaris K1	0.6	0.159

PROCHECK (Laskowski *et al.*, 1993). The volumes of the catalytic cavities were calculated using the *VOIDOO* package (Kleywegt & Jones, 1994). Structure-based sequence alignment of the OXY-1-1 β-lactamase with other β-lactamases was performed using *ClustalW* (Thompson *et al.*, 1997) and drawn using *ESPript* (Gouet *et al.*, 1999). Molecular-graphics illustrations were generated by *PyMOL* (http://www.pymol.org). The surface electrostatic potentials of various β-lactamases were calculated using *PyMOL*. To facilitate comparison with other β-lactamases, the consensus numbering scheme proposed by Ambler *et al.* (1991) was used.

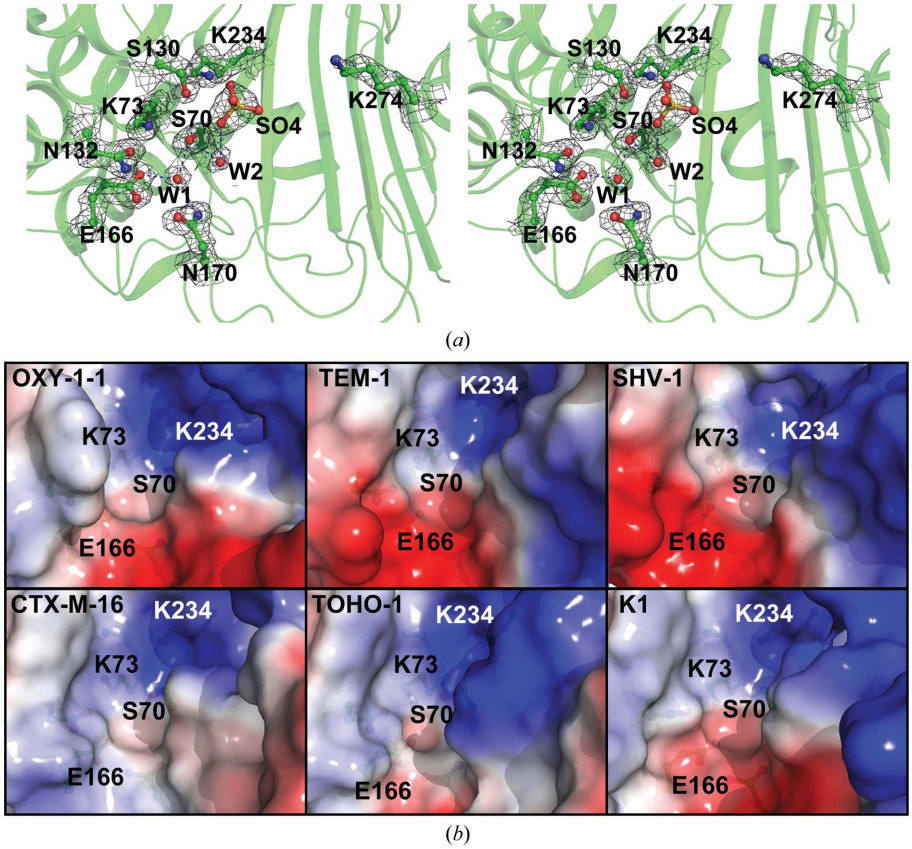

Figure 2
(*a*) Stereoview showing the structure of the active cavity of OXY-1-1 β-lactamase. Highly conserved or catalytically important residues are shown in ball-and-stick representation. Two conserved water molecules and a sulfate ion in the pocket are also shown. The grey mesh shows the $2F_o - F_c$ electron-density map around the highlighted residues and ligands contoured at 1.2σ. (*b*) Surface electrostatic potentials of the substrate-binding pockets of OXY-1-1 and five other β-lactamases; positively and negatively charged regions are represented in blue and red, respectively.

2.3. Penicillin G modelling

The modelling of penicillin G into the active site of the OXY-1-1 β-lactamase was carried out using *UCSF DOCK* (http://dock.compbio.ucsf.edu/). Firstly, the energy of penicillin G was minimized using *CHEMDRAW3D* and this ligand molecule was then docked into the structure of β-lactamase OXY-1-1 by following the tutorials for Flexible Ligand Docking.

3. Results

3.1. Structure determination

The molecular-replacement solution from *CNS* (Brünger *et al.*, 1998) gave an *R* factor of 0.365 for data in the resolution range 15–3 Å after rigid-body refinement. The structure was refined at a resolution of 1.93 Å to an *R* factor of 0.182 and an R_{free} of 0.225; the average *B* factor was 13.30 Å^2 for main-chain atoms and 14.65 Å^2 for side-chain atoms. We point out here from verification of the DNA sequence of the recombinant plasmid and the final electron-density map of the determined structure that the protein prepared in this work was actually the OXY-1-1 β-lactamase instead of the OXY-1a β-lactamase described previously (Wu *et al.*, 2004). The final model consisted of 261 amino-acid residues (28–288; Ambler scheme numbering), 203 water molecules, four sulfate ions and an acetate ion from the crystallization buffer. The N-terminal fragment was not observed (it was disordered without defined electron density). The results of *PROCHECK* showed that the stereochemistry of the final model is reasonable: 90.8% of the residues are in the most favourable region of the Ramachandran plot and no residues are in the disallowed region. The statistics of the refinement are listed in Table 1.

3.2. Overall structure of the OXY-1-1 β-lactamase

The OXY-1-1 β-lactamase exhibited the typical structural architecture of class A β-lactamases composed of two domains: an α/β domain consisting of a five-stranded antiparallel β-sheet with both N- and C-terminal α-helices packed on one side of the sheet and an all-α domain. The catalytic Ser70 is located at the N-terminus of helix α2 in the all-α domain facing the cleft between the two domains (Figs. 1*a* and 1*b*). Structural comparison of the OXY-1-1 β-lactamase and other class A β-lactamases performed with *DaliLite* (Holm & Park, 2000) showed that the

OXY-1-1 β-lactamase structure is quite similar to those of the CTX-M-type ESBLs. The root-mean-square deviations (r.m.s.d.s) for C^{α} atoms between OXY-1-1 and the *E. coli* Toho-1 (PDB entry 1iys; Ibuka *et al.*, 2003), *E. coli* CTX-M-16 (PDB entry 1ylw; Chen *et al.*, 2005) and *Proteus vulgaris* K1 (PDB entry 1hzo; Nukaga *et al.*, 2002) β-lactamases are around 0.6 Å (Table 2). The major structural differences are found in two loop regions on the molecular surface [loops $\alpha2\eta1$ (amino acids 87–91) and $\eta2\alpha3$ (amino acids 112–116); Fig. 1*c*]. The structural differences between OXY-1-1 and the TEM-family and SHV-family β-lactamases are more significant, particularly in the α/β domain. In addition to the surface loops, three helices in the OXY-1-1 α/β domain ($\alpha1$, $\alpha8$ and $\eta4$) shift significantly from their positions in the TEM and SHV β-lactamases (Fig. 1*c*). The r.m.s.d. for C^{α} atoms between OXY-1-1 and the *E. coli* TEM-1 (PDB entry 1tem) and SHV-1 (PDB entry 1shv) β-lactamases are 1.7 and 2.0 Å, respectively (Table 2).

3.3. Catalytic cavity

The structure of the active site is highly conserved among the class A β-lactamases. The catalytic cavity is composed of several motifs. The S*XX*K motif (amino acids 70–73) includes the active Ser residue and occupies the centre of the pocket. The S*X*N motif (amino acids 130–132) from loop $\alpha3\alpha4$ and the KTG motif (amino acids 234–236) in the $\beta3$ strand surround the cavity on both sides. The other side of the cavity is covered by the Ω-loop (amino acids 163–178), in which the Glu166 and Asn170 residues point into the active cavity (Fig. 2*a*). The r.m.s.d.s for the six strictly conserved residues (Ser70, Lys73, Ser130, Asn132, Glu166 and Lys234) between the OXY-1-1 β-lactamase and other class A β-lactamases calculated using *O* (Jones *et al.*, 1990) showed that these residues superimpose quite well (Table 2), indicating that the OXY-1-1 β-lactamase shares a normal-sized catalytic cavity with the CTX-M-type ESBLs and the non-ESBLs TEM and SHV. Indeed, the catalytic cavity volume of the OXY-1-1 β-lactamase is 158 Å^3, which is similar to those of other CTX-M-type ESBLs. Two water molecules (W1 and W2) and a sulfate ion were observed in the active cavity (Fig. 2*a*). The W1 molecule, which is hydrogen-bonded to the side chains of Ser70, Glu166 and Asn170, is conserved in many β-lactamase structures and has been confirmed to be catalytically essential (Adachi *et al.*, 1991). The W2 molecule is found in the oxyanion pocket between the NH groups of Ser70 and Ala237 and forms an additional hydrogen bond to the sulfate ion. The sulfate ion is connected to Ser70, Ser130, Lys234, Thr235, Ala237 and W2 through a hydrogen-bond network and occupies the position of the C3 or C4 carboxylate group of a β-lactam substrate. A notable feature of the OXY-1-1 β-lactamase active site is that its substrate-binding pocket can be clearly divided into two areas based on the surface electrostatic potential distribution: an 'inside' positive area around Lys73 and Lys234 where the sulfate ion is located and an 'outside' negative area around Glu166 (Fig. 2*b*). Similar features also exist in the *P. vulgaris* K1, *E. coli* TEM-1 and *E. coli* SHV-1 β-lactamases, but the negatively and positively charged region profiles are different. The *E. coli* Toho-1 and CTX-M-16 β-lactamases also exhibit different charged region profiles (Fig. 2*b*).

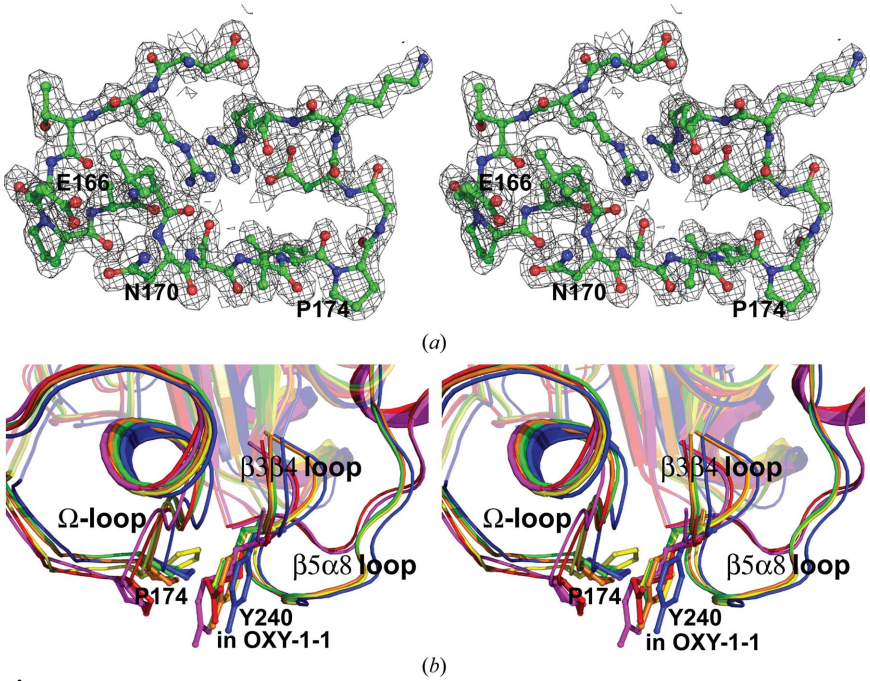

Figure 3
(*a*) Stereoview showing the Ω-loop of OXY-1-1 β-lactamase in ball-and-stick representation outlined with the $2F_o - F_c$ electron-density map contoured at 1.2σ; the positions of Glu166, Asn170 and Pro174 are labelled. (*b*) Stereoview of the superimposition of the Ω-loops of OXY-1-1 and five other β-lactamases. The colour scheme is the same as that in Fig. 1(*c*). The nearby $\beta3\beta4$ and $\beta5\alpha8$ loops are also shown. The Pro174 and Tyr240 residues in OXY-1-1, which show significant structural differences from the other β-lactamases, are shown in stick representation.

3.4. The Ω-loop and other residues near the active site

The Ω-loop has been demonstrated to be essential for the catalytic reaction because the Glu166 and Asn170 side chains point towards and stabilize the position of the conserved W1 in the catalytic pocket. Glu166 also plays a role as a general base in the acylation reaction (Gibson *et al.*, 1990) or as a proton abstractor in the deacylation step (Herzberg & Moult, 1987). In the OXY-1-1 β-lactamase structure the electron density of the Ω-loop is well defined (Fig. 3*a*). The peptide bond between the catalytic Glu166 and the following Pro167 is a conserved *cis* bond. The Ω-loop conformation of OXY-1-1 fits well with those of other CTX-M type β-lactamases, but differs significantly from those of the TEM and SHV β-lactamases. There is a shift of ~2 Å

in the location of Pro174, which is at the tip of the Ω-loop (Fig. 3*b*). Relevant structural changes occur on the opposite side of the interdomain cleft. In the TEM and SHV β-lactamases Arg240 in the $\beta3\beta4$ loop contacts the tip of the Ω-loop, while in OXY-1-1 and other CTX-M-type β-lactamases this residue is replaced by the hydrophobic Tyr. Also, the flat $\beta5\alpha8$ loop is more extended in OXY-1-1 than in the TEM and SHV β-lactamases (Fig. 3*b*).

The OXY-1-1 β-lactamase exhibits differences in amino-acid sequence or conformation from other β-lactamases near the active centre which may also impact on the catalytic properties of the enzyme. Phe72 in the S*XX*K motif (amino acids 70–73) is conserved in the TEM and SHV β-lactamases, but is replaced by a Gly residue in OXY-1-1 (Fig. 1*a*). The hydrophobic environment around the catalytic pocket may be partially complemented by another substitution, Ala135Met (Fig. 1*a*), as the Met side chain points towards the same position as the Phe72 aromatic ring.

Another notable substitution is Trp105 in the $\eta1\eta2$ loop of OXY-1-1; in other β-lactamases this position is occupied by a conserved Tyr. The side chain of Trp105 is observed to point towards the surface of the molecule, while the Tyr side chain in other β-lactamase structures points towards the $\alpha4$ helix (Fig. 4*a*). A penicillin G molecule was modelled in the substrate-binding pocket and it is clearly shown that such a conformation leaves more space near the SDN loop (amino acids 130–132) and provides more hydrophobic protection covering the R_1 substituents of β-lactams.

Positively charged residues at positions 220, 244 or 276, such as Arg244 in the TEM-1 β-lactamase, are involved in substrate binding by interacting with the carboxylate group of the substrate (Jacob-Dubuisson *et al.*, 1991; Zafaralla *et al.*, 1992) and these residues are likely to be involved in the effective binding of inhibitors (Imtiaz *et al.*, 1993, 1994). In the OXY-1-1 β-lactamase a Thr substitutes for Arg244 (Fig. 4*b*), which may have a significant impact on the capability of the enzyme to bind substrates and/or inhibitors.

4. Discussion

The OXY-1-1 β-lactamase shows high structural similarity to other class A β-lactamases, particularly the CTX-M-type β-lactamases. The similarity in both the overall structure and the conserved motifs of the catalytic pocket indicates that the OXY-1-1 β-lactamase follows the general catalytic mechanism of other class A β-lactamases. Unlike non-ESBL enzymes, however, OXY-1-1 has a broad-spectrum substrate profile and exhibits resistance to many inhibitors. The structural features of the enzyme provide a basis for its enzymatic properties.

The catalytic cavity of the OXY-1-1 β-lactamase is of normal size as in the non-ESBL TEM or SHV β-lactamases and other CTX-M-type ESBLs, indicating that it does not broaden the substrate profile by enlarging the active centre. Instead, several residues near the substrate-binding pocket may impact on its interaction with substrate molecules. The positively charged environment between the central β-sheet and the C-terminal $\alpha8$ helix is provided by Lys274 in OXY-1-1 instead of Arg244 as in the TEM-family or SHV-family β-lactamases. The NZ atom of Lys274 in the OXY-1-1 β-lactamase is located at a distance of about 3 Å from the guanidinium group of Arg244 in the TEM-1 β-lactamase, which leaves sufficient space for larger R_2 substituents on the substrates. The positively charged side chains in the vicinity are involved in interaction with the negatively charged carboxylate group of substrates and in effective binding of inhibitors; therefore, the subtle structural changes nearby may affect both the substrate-binding profile and the resistance to inhibitors. Such substitutions and structural features have also been observed in other CTX-M type ESBLs and have been suggested to contribute to the broadened substrate specificity of the enzymes (Nukaga *et al.*, 2002).

Residue Trp105 in the OXY-1-1 β-lactamase is a substitution that is unique to OXY β-lactamases. In TEM, SHV or

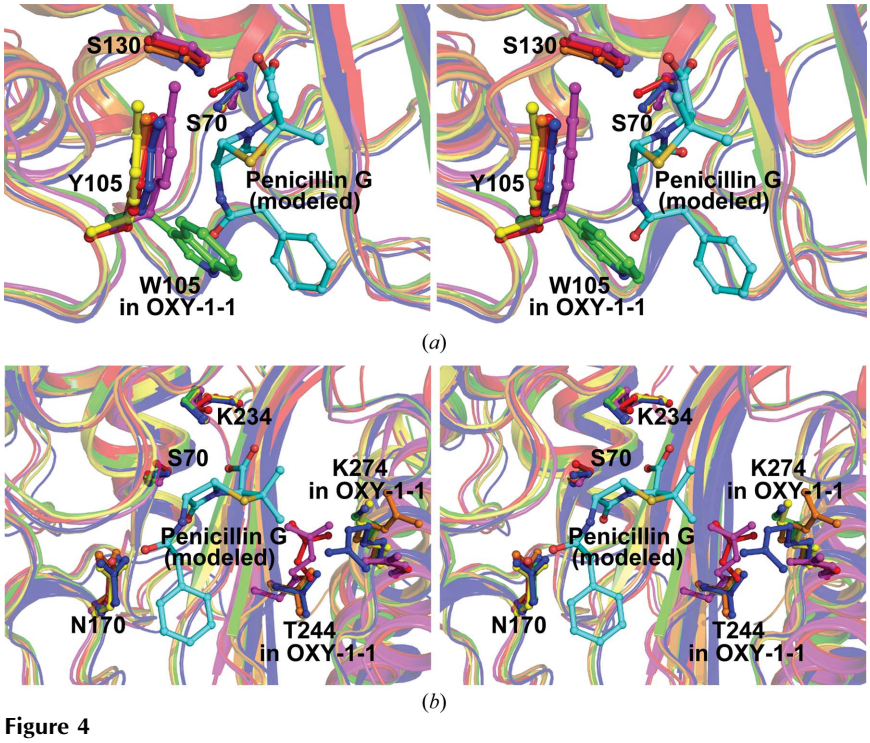

Figure 4
(*a*) Stereoview of comparison around position 105. The colour scheme is the same as in Fig. 1(*c*). Trp105 in OXY-1-1 points in a different direction compared with Tyr105 in other β-lactamases. A penicillin G molecule was modelled in the substrate pocket, indicating the relative position of Trp105 to the R_1 substituent of the substrate. (*b*) Stereoview showing the position of positively charged residues between the substrate-binding pocket and the C-terminal $\alpha8$ helix. The colour scheme is the same as in Fig. 1(*c*). The side chain of Lys274 in the OXY-1-1 β-lactamase points towards the vicinity occupied by Arg244 in the TEM-1 and SHV-1 β-lactamases, with a shift of nearly 3 Å. The R_2 substituent of the modelled penicillin G molecule is located close to the positive group of the Lys274 or Arg244 residue.

CTX-M-type β-lactamases this position is occupied by a strictly conserved Tyr. The structure of the OXY-1-1 β-lactamase showed that the Trp105 side chain points towards the molecular surface instead of the α4 helix that the Tyr side chain points towards in other class A β-lactamases. Such structural differences may leave more space near the SDN loop and provide more hydrophobic protection to R_1 substituents on the substrate molecule. Residue Ser130 plays an essential role in the catalytic reaction as the last proton donor (Lamotte-Brasseur *et al.*, 1991, 1992) and elimination of the Tyr side chain nearby may change the pK_a of Ser130 and hence affect the hydrolysis reaction, but no mutagenesis and enzymatic studies have been reported to date. The Trp105 substitution may also affect the substrate profile, since the hydrophobic environment that it provides may be beneficial to the binding of β-lactams with aromatic R_1 substitutions. In addition, Pro174 at the tip of the Ω-loop in the OXY-1-1 β-lactamase is close to Tyr240 of the $\beta3\beta4$ loop, which also provides more hydrophobic protection to this site. Since the Ω-loop separates the R_1 substituents of β-lactams from the outer hydrophilic environment, the structural features of the OXY-1-1 β-lactamase may be more favourable for the binding of aromatic R_1 substituents than those of the non-ESBL TEM-family and SHV-family enzymes and thus may broaden the substrate specificity of the OXY-1-1 β-lactamase.

The surface electrostatic potential distribution in the substrate-binding pocket of OXY-1-1 may also affect its enzymatic properties. The boundary between the positively and negatively charged areas indicates that the enzyme is apt to bind substrates with charge complementarities. Since the active-site carbonyl group of β-lactam antibiotics is located on the boundary when it is bound to the enzyme, the charge distributions of the R_1 and R_2 substitutions will impact on its binding affinity to the enzyme. Enzymatic assays indicate that the OXY-1-1 β-lactamase has higher hydrolytic activities towards β-lactams with positively charged R_1 substitutions (unpublished work). The difference in hydrolytic activities towards substrates may rely on their binding affinity to the enzyme. The results reported in this study will provide useful clues for the design of more effective β-lactam antibiotics that can resist OXY-family β-lactamases and potential β-lactamase inhibitors targeting OXY-family β-lactamases.

This project was supported by a Fok Ying Tong Education Foundation grant (94017). Peking University's 985 and 211 grants are also greatly acknowledged. We thank the beamline staff of MAX-lab, Lund, Sweden for their kind help with data collection. We also thank Dr Xinhua Ji for critical reading of the manuscript.

References

Adachi, H., Ohta, T. & Matsuzawa, H. (1991). *J. Biol. Chem.* **266**, 3186–3191.
Ambler, R. P. (1980). *Philos. Trans. R. Soc. Lond. B Biol. Sci.* **289**, 321–331.
Ambler, R. P., Coulson, A. F., Frère, J.-M., Ghuysen, J.-M., Joris, B., Forsman, M., Levesque, R. C., Tiraby, G. & Waley, S. G. (1991). *Biochem. J.* **276**, 269–270.
Bonnet, R. (2004). *Antimicrob. Agents Chemother.* **48**, 1–14.
Bonnet, R., Sampaio, J. L. M., Chanal, C., Sirot, D., De Champs, C., Viallard, J. L., Labia, R. & Sirot, J. (2000). *Antimicrob. Agents Chemother.* **44**, 3061–3068.
Bonnet, R., Sampaio, J. L. M., Labia, R., De Champs, C., Sirot, D., Chanal, C. & Sirot, J. (2000). *Antimicrob. Agents Chemother.* **44**, 1936–1942.
Bradford, P. A. (2001). *Clin. Microbiol. Rev.* **14**, 933–951.
Brünger, A. T., Adams, P. D., Clore, G. M., DeLano, W. L., Gros, P., Grosse-Kunstleve, R. W., Jiang, J.-S., Kuszewski, J., Nilges, M., Pannu, N. S., Read, R. J., Rice, L. M., Simonson, T. & Warren, G. L. (1998). *Acta Cryst.* D**54**, 905–921.
Chen, Y., Bonnet, R. & Shoichet, B. K. (2007). *J. Am. Chem. Soc.* **129**, 5378–5380.
Chen, Y., Delmas, J., Sirot, J., Shoichet, B. & Bonnet, R. (2005). *J. Mol. Biol.* **348**, 349–362.
Chen, Y., Shoichet, B. & Bonnet, R. (2005). *J. Am. Chem. Soc.* **127**, 5423–5434.
Davies, J. (1994). *Science*, **264**, 375–382.
Emsley, P. & Cowtan, K. (2004). *Acta Cryst.* D**60**, 2126–2132.
Fevre, C., Jbel, M., Passet, V., Weill, F.-X., Grimont, P. A. D. & Brisse, S. (2005). *Antimicrob. Agents Chemother.* **49**, 3453–3462.
Fournier, B., Arlet, G., Lagrange, P. H. & Philippon, A. (1994). *FEMS Microbiol. Lett.* **116**, 31–36.
Fournier, B., Lagrange, P. H. & Philippon, A. (1996*a*). *Antimicrob. Agents Chemother.* **40**, 460–463.
Fournier, B., Lagrange, P. H. & Philippon, A. (1996*b*). *J. Antimicrob. Chemother.* **37**, 931–942.
Fournier, B., Lu, C. Y., Lagrange, P. H., Krishnamoorthy, R. & Philippon, A. (1995). *Antimicrob. Agents Chemother.* **39**, 1365–1368.
Fournier, B., Roy, P. H., Lagrange, P. H. & Philippon, A. (1996). *Antimicrob. Agents Chemother.* **40**, 454–459.
Frère, J.-M. (1995). *Mol. Microbiol.* **16**, 385–395.
Ghuysen, J.-M. (1991). *Annu. Rev. Microbiol.* **45**, 37–67.
Gibson, R. M., Christensen, H. & Waley, S. G. (1990). *Biochem. J.* **272**, 613–619.
Gouet, P., Courcelle, E., Stuart, D. I. & Métoz, F. (1999). *Bioinformatics*, **15**, 305–308.
Granier, S. A., Leflon-Guibout, V., Goldstein, F. W. & Nicolas-Chanoine, M.-H. (2003). *Antimicrob. Agents Chemother.* **47**, 2922–2928.
Hart, C. A. (1993). *J. Hosp. Infect.* **23**, 83–86.
Herzberg, O. & Moult, J. (1987). *Science*, **236**, 694–701.
Holm, L. & Park, J. (2000). *Bioinformatics*, **16**, 566–567.
Ibuka, A. S., Ishii, Y., Galleni, M., Ishiguro, M., Yamaguchi, K., Frère, J.-M., Matsuzawa, H. & Sakai, H. (2003). *Biochemistry*, **42**, 10634–10643.
Ibuka, A., Taguchi, A., Ishiguro, M., Fushinobu, S., Ishii, Y., Kamitori, S., Okuyama, K., Yamaguchi, K., Konno, M. & Matsuzawa, H. (1999). *J. Mol. Biol.* **285**, 2079–2087.
Imtiaz, U., Billings, E., Knox, J. R., Manavathu, E. K., Lerner, S. A. & Mobashery, S. (1993). *J. Am. Chem. Soc.* **115**, 4435–4442.
Imtiaz, U., Billings, E. M., Knox, J. R. & Mobashery, S. (1994). *Biochemistry*, **33**, 5728–5738.
Jacob-Dubuisson, F., Lamotte-Brasseur, J., Dideberg, O., Joris, B. & Frère, J.-M. (1991). *Protein Eng.* **4**, 811–819.
Jones, T. A., Bergdoll, M. & Kjeldgaard, M. (1990). *Crystallographic and Modeling Methods in Molecular Design*, edited by C. Bugg & S. Ealick, pp. 189–195. Berlin: Springer-Verlag.
Kimura, S., Ishiguro, M., Ishii, Y., Alba, J. & Yamaguchi, K. (2004). *Antimicrob. Agents Chemother.* **48**, 1454–1460.
Kleywegt, G. J. & Jones, T. A. (1994). *Acta Cryst.* D**50**, 178–185.

Knox, J. R. (1995). *Antimicrob. Agents Chemother.* **39**, 2593–2601.
Lamotte-Brasseur, J., Dive, G., Dideberg, O., Charlier, P., Frère, J.-M. & Ghuysen, J.-M. (1991). *Biochem. J.* **279**, 213–221.
Lamotte-Brasseur, J., Jacob-Dubuisson, F., Dive, G., Frère, J.-M. & Ghuysen, J.-M. (1992). *Biochem. J.* **282**, 189–195.
Laskowski, R. A., MacArthur, M. W., Moss, D. S. & Thornton, J. M. (1993). *J. Appl. Cryst.* **26**, 283–291.
Levy, S. B. (1994). *Trends Microbiol.* **2**, 341–342.
Livermore, D. M. (1995). *Clin. Microbiol. Rev.* **8**, 557–584.
Matagne, A., Lamotte-Brasseur, J. & Frère, J.-M. (1998). *Biochem. J.* **330**, 581–598.
Murshudov, G. N., Skubák, P., Lebedev, A. A., Pannu, N. S., Steiner, R. A., Nicholls, R. A., Winn, M. D., Long, F. & Vagin, A. A. (2011). *Acta Cryst.* D**67**, 355–367.
Nukaga, M., Mayama, K., Crichlow, G. V. & Knox, J. R. (2002). *J. Mol. Biol.* **317**, 109–117.
Orencia, M. C., Yoon, J. S., Ness, J. E., Stemmer, W. P. C. & Stevens, R. C. (2001). *Nature Struct. Biol.* **8**, 238–242.
Painter, J. & Merritt, E. A. (2006). *Acta Cryst.* D**62**, 439–450.
Podschun, R. & Ullmann, U. (1998). *Clin. Microbiol. Rev.* **11**, 589–603.
Poirel, L., Weldhagen, G. F., Naas, T., De Champs, C., Dove, M. G. & Nordmann, P. (2001). *Antimicrob. Agents Chemother.* **45**, 2598–2603.
Shimizu-Ibuka, A., Matsuzawa, H. & Sakai, H. (2004). *Biochemistry*, **43**, 15737–15745.
Thompson, J. D., Gibson, T. J., Plewniak, F., Jeanmougin, F. & Higgins, D. G. (1997). *Nucleic Acids Res.* **25**, 4876–4882.
Tzouvelekis, L. S., Tzelepi, E., Tassios, P. T. & Legakis, N. J. (2000). *Int. J. Antimicrob. Agents*, **14**, 137–142.
Wang, X., Minasov, G. & Shoichet, B. K. (2002). *J. Mol. Biol.* **320**, 85–95.
Winn, M. D. (2011). *Acta Cryst.* D**67**, 235–242.
Wu, S. W. (1998). PhD thesis. Karolinska Sjukhuset, Stockholm, Sweden.
Wu, S. W., Dornbusch, K., Göransson, E., Ransjö, U. & Kronvall, G. (1991). *J. Antimicrob. Chemother.* **28**, 389–397.
Wu, S. W., Dornbusch, K., Norgren, M. & Kronvall, G. (1992). *J. Antimicrob. Chemother.* **30**, 3–16.
Wu, S. W., Liang, Y.-H. & Su, X.-D. (2004). *Acta Cryst.* D**60**, 326–328.
Zafaralla, G., Manavathu, E. K., Lerner, S. A. & Mobashery, S. (1992). *Biochemistry*, **31**, 3847–3852.